

# Kinetic Analysis and CFD Modelling of Hydrogen-Air Combustion Applied to Scramjet Vehicles

Guido Saccone<sup>1</sup>, Pasquale Natale<sup>1</sup>, Luigi Cutrone<sup>1</sup>, Marco Marini<sup>1</sup>

<sup>1</sup>CIRA (Italian Aerospace Research Centre)

Via Maiorise snc, 81043 Capua (CE), Italy

[g.saccone@cira.it](mailto:g.saccone@cira.it); [p.natale@cira.it](mailto:p.natale@cira.it); [l.cutrone@cira.it](mailto:l.cutrone@cira.it); [m.marini@cira.it](mailto:m.marini@cira.it)

**Abstract** - In the field of air-breathing hypersonic scramjet vehicles design and development, the Italian Aerospace Research Centre – CIRA has contributed to an international project, called Stratospheric Flying Opportunities for High-Speed Propulsion Concepts – STRATOFLY, in collaboration with several European organizations, coordinated by Politecnico di Torino under the EC Horizon 2020 programme financial support. Aim of this project was the improvement of enabling technologies for realization of a commercial hypersonic aircraft, able to flight at Mach 8, at 30÷35 km of altitude, for at least 4 hours with a minimum environmental impact and especially low NO<sub>x</sub> emissions. Understanding the complex, supersonic, turbulent, combustion processes occurring during scramjet operations is of fundamental importance. For this purpose, a thorough 0D kinetic assessment was carried out by means of the open-source Cantera software for identification of the most suitable kinetic mechanisms, able to predict with a satisfactory accuracy both the ignition delay times and the NO<sub>x</sub> emissions at the relevant scramjet operating conditions. Several kinetic schemes were investigated and the computed results were compared with the literature available shock tubes and rapid compression machines experimental data. In the entire investigated operative box, the best agreement, in terms of induction times, was achieved using the kinetic mechanism developed by Zettervall and Fureby. Moreover, for considering the generation of NO<sub>x</sub>, the three fundamental thermal route reactions by Zel'dovič, was added. Furthermore, full 3D CFD simulations were carried out in Ansys<sup>®</sup> Fluent in order to compare experimental data and evaluate predictivity of such kinetic mechanisms. For the sake of comparison, the experiments carried out on the small-scale scramjet vehicle of LAPCAT-II by the HEG (DLR) were rebuilt.

**Keywords:** scramjet, hypersonic flight, hydrogen combustion, kinetic analysis, CFD

## 1. Introduction

Civil hypersonic, scramjet, trans-atmospheric transportation is becoming increasingly central in the global economy in order to connect passengers and goods between terrestrial antipodal hubs in few hours.

On this purpose, hydrogen is a promising candidate as fuel for hypersonic air-breathing, long-term passenger transportation vehicles, because it can be burned in an efficient and reliable manner in supersonic combustion engines [1].

Furthermore, H<sub>2</sub> is esteemed as a clean fuel with lower environmental impact compared to hydrocarbons, since the overall product of its complete oxy-combustion is only water, even if, when reacts with air, it produces also NO<sub>x</sub>, due to the elevated flame temperatures, reached during combustion. However, a comprehensive understanding of the supersonic hydrogen/air combustion could allow optimized design of the combustion chamber able to decrease the flame temperatures and consequently the pollutant NO<sub>x</sub> emissions.

Hydrogen combustion is a very challenging process, consisting in several critical phenomena i.e., injection, compressible mixing, chemical kinetics, ignition, flame holding, vortices generation, turbulence combustion modelling, interactions among shock waves, boundary layer and heat release, etc. Moreover, scramjet operation is further complicated by the very short residence time ( $\sim 10^{-3}$  s) of the flow through the combustor chamber that is of the same order of magnitude of chemical kinetic ignition time of stoichiometric hydrogen/air mixtures at the typical conditions of scramjet combustion. Since experimental investigations is often unfeasible due to several difficulties in measuring multispecies, reacting, high-speed, unsteady flow fields [1], the most convenient way for design and development of scramjet vehicles relies on CFD modelling and simulations.

Hydrogen/air kinetic mechanisms assessment is an important, preliminary task for the development of physical-chemical combustion models to be implemented into CFD codes. The optimal scheme arises as suitable trade-off between the accuracy, required for a reliable description of ignition and combustion phenomena and the computational costs, associated to the available calculation speed and memory storage capacity. For this purpose, a preliminary zero-

dimensional kinetic analysis of hydrogen/air combustion at the most relevant operative conditions for this application was performed using the three most suitable kinetic mechanisms i.e., Jachimowski – 1988 [2], Kéromnès – 2013 [3] and Z25 - Zettervall – 2018 [4], previously selected on the basis of the review of Gerlinger et al. [5] and Olm and co-workers [6].

In addition, full 3D CFD analyses are carried out in order to compare experimental data and evaluate predictivity of such kinetic schemes. In particular, a reduced version of Jachimowski scheme [7] was compared to the scheme developed by Zettervall.

## 2. Methods

Time-dependent 0D simulations of homogeneous, isochoric and adiabatic batch reactors, filled with premixed, gaseous, reacting hydrogen/air mixtures were carried out using the kinetic and thermodynamic open-source Cantera software [8] under Python interface and the three investigated mechanisms i.e., Jachimowski – 1988 [2], Kéromnès – 2013 [3] and Z\_25 - Zettervall – 2018 [4].

The mathematical-chemical model consists in the following fundamental mass and energy balance equations:

$$m_{tot} = \sum_{k=1}^K m_k = const. \Leftrightarrow \frac{dm_{tot}}{dt} = 0 \quad (1)$$

$$\frac{dm_k}{dt} = V r_k M_{w,k} \quad (2)$$

$$c_p \frac{dT}{dt} + v \cdot \sum_{k=1}^K h_k \cdot r_k \cdot M_{w,k} = 0 \quad (3)$$

where  $m_{tot}$ ,  $V$ ,  $T$ ,  $c_p$  are respectively the total mass, volume, temperature and the specific heat at constant pressure of the reacting mixture, while  $m_k$ ,  $h_k$  and  $M_{w,k}$  the mass, the enthalpy and the molecular weight of the generic  $k$  chemical substance,  $r_k$  is the reaction rate and  $v$  the stoichiometric coefficient.

The initial temperature, pressure and equivalence ratios for every 0D simulations were selected according to the literature available shock tube and Rapid Compression Machine - RCM experiments and the gaseous reacting mixture was evaluated using the ideal gas law.

### 2.1. Jachimowski – 1988

It is a detailed mechanism, consisting in 13 chemical species and 33 reactions formulated using the experimental data collected in the shock-tube and laminar flame tests, carried out at NASA - Langley Research Center in the framework of the American National Aero-Space Plane – NASP with the aim to investigate hydrogen/air combustion for propulsion systems of vehicles able to operate at flight speed up to Mach 25 [2].

It includes all the main atomic, radical and molecular species of the hydrogen-oxygen-nitrogen system relevant at elevated Mach number conditions ( $M > 12$ ) i.e.,  $H_2$ ,  $O_2$ ,  $H$ ,  $O$ ,  $OH$ ,  $H_2O$ ,  $HO_2$ ,  $H_2O_2$ ,  $N$ ,  $NO$ ,  $HNO$ . Moreover, this mechanism was refined, through comparison between calculated and experimental kinetic data. Therefore, rate coefficients for certain reactions were adjusted in order to obtain the best agreement with the experimental measurements of real hydrogen-air mixtures i.e., ignition delay times reported by Slack [8] and laminar burning velocities of Warnatz [9] and Milton and Keck [10]. Other available experimental data were discarded because achieved for diluted e.g.,  $H_2$ - $O_2$ -Ar mixtures.

### 2.2. Kéromnès – 2013

This is a detailed kinetic mechanism suitably conceived for investigating the oxidation of syngas mixture consisting in  $H_2/CO/O_2/N_2/Ar$  at pressures from 1 to 70 bar, over a temperature range of 900-2550 K and equivalence

ratios from 0.1 to 4 [3]. As listed in Table 2, this kinetic scheme involves 12 chemical species comprising also the excited radical OH\* and interacting among them through 33 reversible reactions.

Kéromnès and co-workers [3] concerning hydrogen ignition under high pressure and intermediate temperature conditions noticed a key role played by the following fundamental reactions i.e., [R17]  $\text{H}_2 + \text{HO}_2 \leftrightarrow \text{H} + \text{H}_2\text{O}_2$  and [R15]  $\text{H}_2\text{O}_2 (+\text{M}) \leftrightarrow \text{OH} + \text{OH} (+\text{M})$ .

According to the authors [3], hydrogen reactivity is mainly controlled by the competition between the chain-branching reaction [R1]  $\text{H} + \text{O}_2 \leftrightarrow \text{O} + \text{OH}$  and the pressure-dependent chain-propagating reaction: [R9]  $\text{H} + \text{O}_2 (+\text{M}) \leftrightarrow \text{HO}_2 (+\text{M})$ .

For this reason, [R1] and [R9] reactions were extensively investigated. Under the low to intermediate temperatures (< 1000 K) usually encountered in the Rapid Compression Machines – RCM, hydrogen oxidation is predominantly governed by reaction [R9], which leads to production of hydroperoxyl radical i.e., HO<sub>2</sub>. It reacts with molecular hydrogen generating H<sub>2</sub>O<sub>2</sub> according to reaction [R17]. Finally, oxygenated water decomposes to two OH radical as prescribed by reaction [R15].

Instead at the high temperatures experienced by shock tube equipment, the competition between [R1] and [R9] leads to a pressure dependence of ignition delay times. Indeed, depending on the pressure, at high temperatures the oxidation process is mainly controlled by reaction [R1].

### 2.3. Z25 – Zettervall - 2018

This is a detailed, hydrogen/oxygen kinetic mechanism consisting in 9 species and 22 irreversible elementary reactions [4]. In addition, since the considered oxidizer is ambient air, the scheme also includes the three following Zel'dovič thermal route reversible reactions [11], leading to production of NO were added: [R23]  $\text{N} + \text{NO} \leftrightarrow \text{N}_2 + \text{O}$ ; [R24]  $\text{N} + \text{O}_2 \leftrightarrow \text{NO} + \text{O}$  and [R25]  $\text{N} + \text{OH} \leftrightarrow \text{NO} + \text{H}$ .

It arises the H<sub>2</sub>-O<sub>2</sub> chemical structure from [12] with three additional fuel breakdown reactions from [13] and [14].

Analogously to Kéromnès et al. [3], also Zettervall and Fureby [4] highlight the importance of the competition between the chain-branching reaction [R4]:  $\text{H} + \text{O}_2 \rightarrow \text{OH} + \text{O}$  and the chain-propagating reaction [R12]:  $\text{H} + \text{O}_2 (+\text{M}) \rightarrow \text{HO}_2 (+\text{M})$ . The first creates a pool of radical species effectively decreasing the ignition time, while the second produces the hydroperoxyl radical, which inhibit the chain-branching combustion process and therefore increases the induction time. The competition between these reactions and the consequent distribution of fast i.e., O, H and OH radicals and the slow radical HO<sub>2</sub> is strongly temperature dependent. Furthermore, in the P-T diagram a region of rapid ignition corresponding to chain-branching explosion at high temperatures and a region of slow ignition, associated to the thermal explosion at low temperatures are separated by a crossover region, corresponding to intermediate temperatures and dominated by extremely complex chemical processes. However, for instance, several ramjets, scramjets and dual mode engines operate exactly in this connecting, critical zone.

Z25 includes reactions important for the complete temperature spectrum, below and above the crossover region. In the mechanism development, authors spent particular efforts for improving its capability to match the ignition experimental behaviour also in the intermediate connecting region, because it is extremely useful for ensuring flame anchoring and the stabilization within the supersonic combustion engines.

At low temperatures, reaction [R12] predominates over reaction [R4] and the HO<sub>2</sub> concentration enhances and new reaction paths become more important i.e., [R16]:  $\text{HO}_2 + \text{HO}_2 \rightarrow \text{H}_2\text{O}_2 + \text{O}_2$  and [R20]:  $\text{H}_2\text{O} + \text{HO}_2 \rightarrow \text{H}_2\text{O}_2 + \text{OH}$ . These reactions increase the concentration of H<sub>2</sub>O<sub>2</sub>, which main consumption route is carried out by means of reaction [R17]:  $\text{H}_2\text{O}_2 (+\text{M}) \rightarrow \text{OH} + \text{OH} (+\text{M})$ , that produces two OH radicals, which in turn generate H radical through [R8]:  $\text{H}_2 + \text{OH} \rightarrow \text{H}_2\text{O} + \text{H}$ . The new, so developed, kinetic mechanism was labelled Z25.

## 2.4. Comparison against experimental data

This section presents the comparison between the computational ignition delay times, calculated as described in the previous paragraph using the three investigated kinetic mechanisms and the corresponding experimental data associated to the same initial temperature, pressure and equivalence ratios, provided by several researchers and measured within shock tube and/or RCM tests.

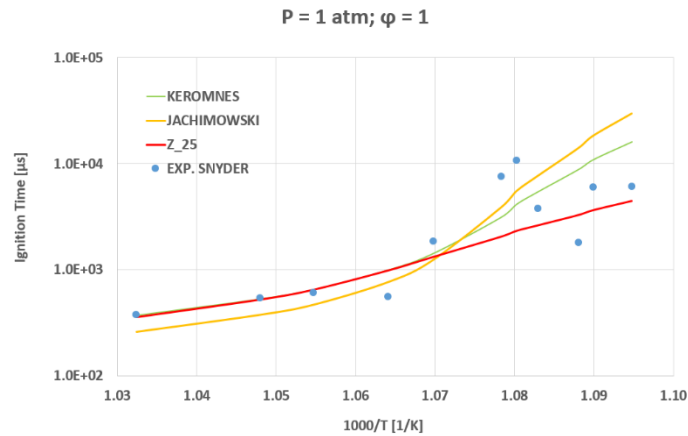


Fig. 1: Calculated ignition delay times against Snyder [15] experimental data at  $p = 1$  atm.

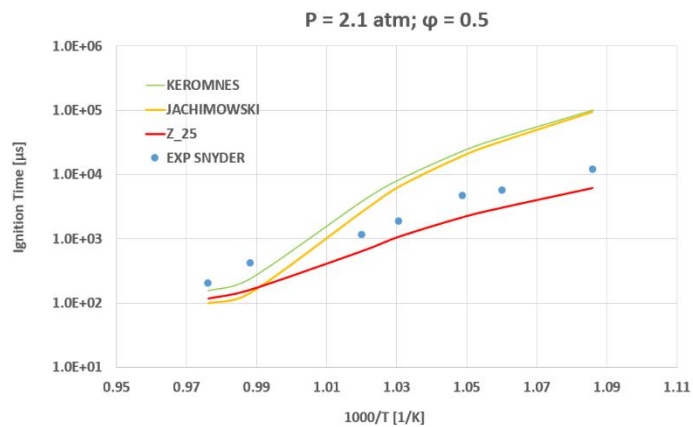


Fig. 2: Calculated ignition delay times against Snyder [15] experimental data at  $p = 1$  atm.

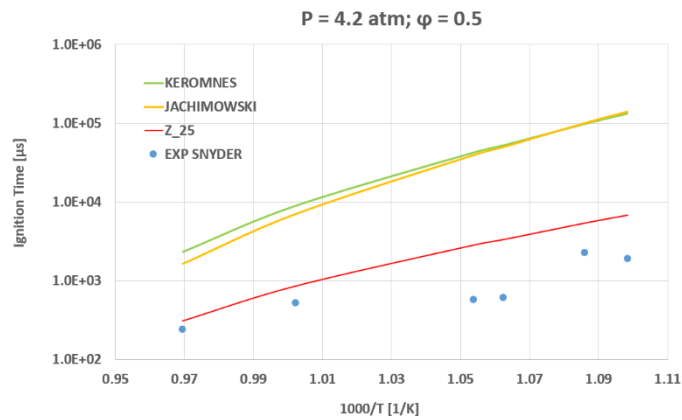


Fig. 3: Calculated ignition delay times against Snyder [15] experimental data at  $p = 4.2$  atm.

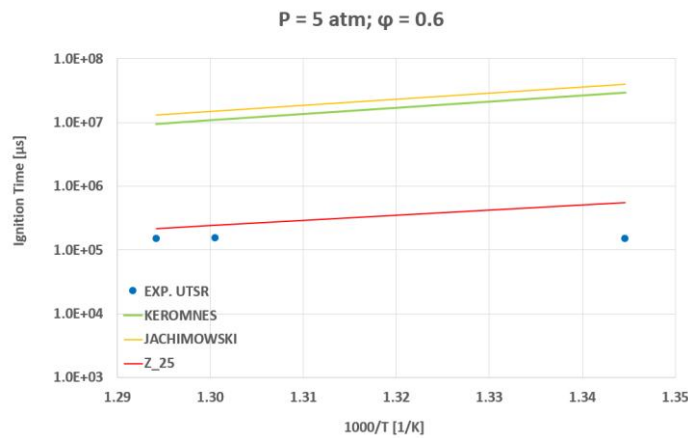


Fig.4. Calculated ignition delay times against UTSR experimental data at  $p = 5$  atm.

In the investigated operative box, the best agreement between computational and experimental data was achieved by the Z25 kinetic mechanism.

The matching of Jachimowski – 1988 [2] and Kéromnés – 2013 [3] kinetic schemes are satisfactory only for high temperatures and low pressures, while in the crossover region, associated to intermediate-low temperatures and pressure above 2 bar only the Z25 [4] provides a quite good behaviour.

Based on the present data, the most suitable kinetic mechanism to be embedded in mathematical models for CFD simulations of supersonic combustion in ramjets, scramjets and dual mode engines is exactly the scheme by Zettervall and Fureby [8] including also the three fundamental NO generation reactions by Zel'dovič [11].

### 2.3. CFD Results

During STRATOFly programme, a ground-based testing of small-scale version of LAPCAT-II M8 vehicle was successfully tested in HEG wind tunnel at the German Aerospace Center - DLR [16]. By the test campaign, several experimental data were collected, useful for exp-CFD comparison. CFD run was performed by Ansys Fluent®.

In Fig. 5, experimental data are reported as square dots. Different colours represent different acquisition lines: intake line, on the middle section of the intake; chamber line, on the side of the combustion chamber; nozzle line, on the middle section of the expansion nozzle. In order to perform faster CFD simulations, the vehicle geometry was simplified. In particular, the intake was removed and only combustion process, along with nozzle expansion, was simulated. In order to decrease the CFD computational cost, the numerical domain was simplified removing the intake. Moreover, taking

advantage of symmetry of the boundary condition, only one half of the vehicle was considered. Since only combustion chamber and nozzle are considered, it was not possible to apply wind tunnel condition to the inlet of the computational domain. The inlet was directly applied at the initial section of the combustion chamber ( $X=0.41$  in Fig. 5). For this reason, in the figure, the CFD results (represented by continuous lines) start from this section. In the figure, triangle dots represent the solution obtained by means of the reduced version of Jachimowski scheme [7]. While, circle dots represent the solution obtained by means of Zettervall one. The two schemes are quite similar.

An unexpected compression occurs just after the inlet. This compression is a consequence of the abrupt temperature increasing caused by the combustion process. Thus, even if the comparison between CFD and EXP is not agreed along the axial ( $X$  coordinate) distribution, the predicted pressure value is consistent with the experimental measurement. This enables both kinetic schemes (JR as well as Z25) to be accountable for 3D CFD simulations of the  $H_2-O_2$  combustion.

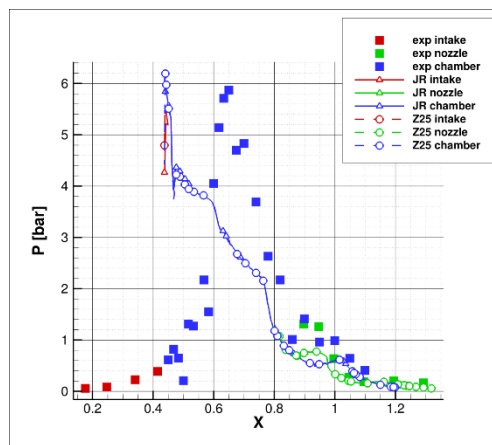


Fig. 5: Pressure distribution along experimental line acquisition. Jachimowski (JR) vs. Zettervall (Z25) comparison.

In Fig. 6, the temperature contour plot is reported over some slices of the combustion chamber. This solution relates to JR solution reported in Fig. 5. In order to better understand temperature distribution, iso-surface of 20% mass-fraction of fuel (hydrogen) is also reported. The CFD run was carried out using Eddy Dissipation Concept as combustion model, along with a standard  $k-\epsilon$  turbulence model and 2<sup>nd</sup> order up-wind discretization scheme.

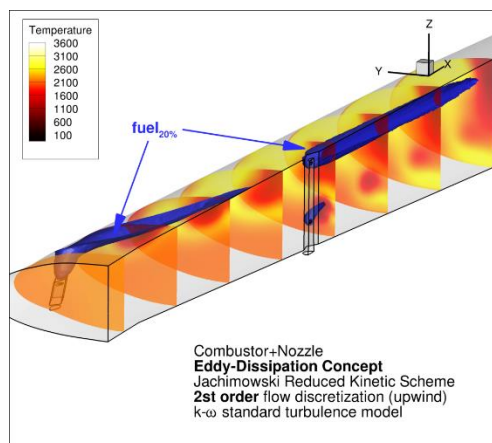


Fig. 6: Temperature contour plot over cross-sectional slices of the combustion chamber.

### 3. Conclusion

The hydrogen/air supersonic combustion process was analysed both on chemical kinetic and computational fluid dynamic points of view.

A 0D kinetic assessment in the operative conditions experienced in scramjet engines was carried out on literature available combustion mechanisms and the best agreement with experimental shock ignition delay times measurements was achieved with Z25 scheme especially conceived for capturing the complex reaction paths followed by the radical pools in the crossover region at moderate pressure and intermediate temperatures.

The fully-3D CFD simulations confirmed that kinetic schemes due to Zettervall [4] and Jachimowski [7] are quite good for pressure predictions when hydrogen/oxygen combustion is under investigation.

### Acknowledgements

The H2020 STRATOFly Project has received funding from the European Union's Horizon 2020 research and innovation programme under Grant Agreement No. 769246.

### References

- [1] D. Cecere, A. Ingenito, E. Giacomazzi, L. Romagnosi, and C. Bruno, "Hydrogen/air supersonic combustion for future hypersonic vehicles," *International Journal of Hydrogen Energy*, vol. 30, pp. 1-16, 2011.
- [2] C. J. Jachimowski, "An Analytical Study of the Hydrogen-Air Reaction Mechanism With Application to Scramjet Combustion," NASA Technical Paper 2791, 1988.
- [3] A. Kéromnès, W. K. Metcalfe, K. A. Heufer, N. Donohoe, C. J. Sung, J. Herzler, C. Naumann, P. Griebel, O. Mathieu, M. C. Krejci, E. L. Petersen, W. J. Pitz, H. J. Curran, and A. K. Das, "An Experimental and Detailed Chemical Kinetic Modelling Study of Hydrogen and Syngas Mixtures at Elevated Pressures," *Combustion and Flame*, 2013.
- [4] N. Zettervall, and C. Fureby, "A Computational Study of Ramjet, Scramjet and Dual Mode Ramjet/Scramjet Combustion in a Combustor with a Cavity Flameholder," *Proceedings of AIAA Aerospace Science Meeting Kissimmee*, 8-12 January (2018), Florida (U.S.A.).
- [5] P. Gerlinger, K. Nold, and M. Aigner, "Investigation of Hydrogen-Air Reaction Mechanisms for Supersonic Combustion," 44th AIAA/ASME/SAE/ASEE Joint Propulsion Conference & Exhibit, 21 – 23 July 2008, Hartford, U.S.A.
- [6] C. Olm, I. G. Zsély, R. Pálvölgyi, T. Varga, T. Nagy, H. J. Curran, and T. Turányi, "Comparison of the performance of several recent hydrogen combustion mechanisms," *Combustion and Flame*, vol. 161, pp. 2219-2234, 2014.
- [7] J. B. Star, "Numerical Simulation of Scramjet Combustion in a Shock Tunnel", Ph.D. Dissertation, Dept. Aerospace Engineering North Carolina State University.
- [8] D. Goodwin, H. K. Moffat, and R. L. Speth, "Cantera: An Object-oriented Software Toolkit for Chemical Kinetics, Thermodynamics, and Transport Processes," (Version 2.6) [Online]. Available: <http://www.cantera.org>.
- [9] J. Warnatz, "Concentration-, Pressure-, Temperature-Dependence of the Flame Velocity in Hydrogen-Oxygen-Nitrogen Mixtures," *Combustion Science and Technology*, vol. 26, no. 5-6, 1981.
- [10] B.E. Milton and J. C. Keck, "Laminar Burning Velocities in Stiochiometric Hydrogen and Hydrogen-Hydrocarbon Gas Mixtures, *Combustion and Flame*, vol. 58, pp. 13-22, 1984.
- [11] Y.B. Zel'dovič, "The Oxidation of Nitrogen in Combustion Explosions", *Acta Physicochimica* 21, 577–628, (1946).
- [12] A. Larsson, N. Zettervall, T. Hurtig, E. J. K. Nilsson, A. Ehn, P. Petersson, M. Alden, J. Larfeldt. and C. Fureby, "Skeletal Methane-Air Reaction Mechanism for Large Eddy Simulation of Turbulent Microwave-Assisted Combustion," *Energy Fuels*, vol. 31, pp.1904, 2017.
- [13] M. Ó Conaire, H. J. Curran, J. M. Simmie, W. J. Pitz, and C. K. Westbrook, "A Comprehensive Modeling Study of Hydrogen Oxidation," *Interscience.wiley.com*, 2004.

- [14] V. A. Alekseev, M. Christensen, and A. A. Konnov, "The Effect of Temperature on the Adiabatic Burning Velocities of Diluted Hydrogen Flames: A Kinetic Study using an Updated Mechanism," *Combustion and Flame*, vol. 162, pp. 1884, 2015.
- [15] A. D. Snyder, J. Robertson, D. L. Zanders, G. B. Skinner, Technical Report Monsanto Research Corporation Dayton Ohio, (1965).
- [16] K. Hannemann, J. M. Schramm, S. Karl, S. J. Laurence, "Free Flight Testing of a Scramjet Engine in a Large Scale Shock Tunnel", AIAA 2015-3608, Session: Propulsion Systems V, Jul 2015.